JOURNAL OF MATERIALS SCIENCE **35** (2000) 1453–1458

Effect of Ta_2O_5 doping on the electrical properties of $0.99SnO_2 \cdot 0.01CoO$ ceramic

A. C. ANTUNES, S. M. ANTUNES, S. A. PIANARO
Universidade Estadual de Ponta Grossa 84031-510 Ponta Grossa, PR, Brazil

E. LONGO
Departamento de Química, Universidade Federal de São Carlos, 13560-905 São Carlos SP, Brazil
E-mail: dels@power.ufscar.br

J. A. VARELA
Instituto de Química, Universidade Estadual Paulista, 14801-970, Araraquara, SP, Brazil

The effect of Ta_2O_5 doping in $0.99SnO_2 \cdot 0.01CoO$ on the microstructure and electrical properties of this ceramic were analyzed in this study. The grain size was found to decrease from 6.87 μm to 5.68 μm when the Ta_2O_5 concentration increased from 0.050 to 0.075 mol%. DC electrical characterization showed a dramatic increase in the current loss and decrease in the non-linear coefficient with the increase of the Ta_2O_5 concentration. The conduction mechanism is by thermionic emission and the potential barriers are of Schottky type, separated by a thin film.

1. Introduction

Tin dioxide (SnO_2) is an n type wide band gap semiconductor with crystalline structure of rutile type and has a low densification rate due to its high surface diffusion at low temperatures and high SnO_2 partial pressure at high temperatures [1]. Dense SnO_2 based ceramics can be achieved by introducing dopants [2–5] or by pressure assisted sintering [6, 7]. Dopants with valence $+2$ can promote densification of SnO_2 ceramics due to formation of a solid solution with creation of oxygen vacancies.

In a former study [8, 9] we have shown that the CoO and Nb_2O_5 doped SnO_2 ceramic is single phase and presents varistor behavior with $\alpha = 8.0$. By adding 0.05 mol% of Cr_2O_3 the system still is a single phase with the non linear coefficient increasing to $\alpha = 41$ [10].

The electric behavior of varistors is governed by the presence of voltage barriers at the grain boundaries [11, 12]. For a given varistor system each voltage barrier is characterized by a specific value v_b. Considering the SnO_2 varistor microstructure, a Schottky type electrical barrier can be ascribed to be the most likely barrier at the SnO_2 grain boundary since no intergranular insulating layer separating two SnO_2 grains was observed. The negative surface charge at the grain boundary interface is compensated by the positive charge in the grain depletion layer on both sides of interface [11].

The role of Nb_2O_5 or Ta_2O_5 in the SnO_2 ceramics is to increase the electronic conductivity of this ceramics as reported by Las *et al.* [13]. We have shown recently that the substitution of 0.05 mol% of Nb_2O_5 by Ta_2O_5 in the CoO doped SnO_2 ceramics increases the non-linear coefficient from 8 to 13 [14]. The effect of small additions of Ta_2O_5 on the electric properties of 1.0 mol% CoO doped SnO_2 is investigated in this study.

2. Experimental procedure

Reagent grades SnO_2 (Merck), CoO (Riedel) and Ta_2O_5 (Merck) powders were used to prepare the SnO_2 based ceramic. The following compositions (all in mole%) were prepared using the above oxides: (1) $0.99\ SnO_2 \cdot 0.01\ CoO + 0.05$ mol% Ta_2O_5, and (2) $0.99\ SnO_2 \cdot 0.01\ CoO + 0.075$ mol% Ta_2O_5.

The powders with the above compositions were ball milled with zirconia balls in isopropyl alcohol media inside of a polypropylene jar during 18 h. Then the powder was dried, inside an oven, at 100°C during 4 h. The resulting powders were granulated in a 200 mesh sieve and uniaxialy pressed (in cylindrical shape 13.0 mm diameter and 1.3 height) at 100 MPA reaching 55% of the theoretical density (green density of 3.82 g/cm^3).

Sintering of the pellets were performed in a tube furnace at 1300°C during 2 h. The furnace was heated to 1300°C by using heating rate of 3°C/min and cooled down using the same rate.

For microstructure analysis the samples were polished using sand paper and alumina powder and then thermally etched at 1250°C during 15 minutes. A JEOL (JSM T330A model) scanning electron microscope was used for microstructure observations. Mean grain size, D, was determined by using the equation proposed by Mendelson [15], $D = 1.558L$, where L is the average intercept number between a series of random lines, drawn in the micrograph, with the grain boundaries. Crystalline phases were determined by using x-ray

Diffraction (SIEMES model D-5000). A stabilized voltage source (TECTROL model TCH 3000-2) and two digital multimeters (FLUKE 8050 A) were used for electrical characterization of the samples. The sintered pellets were sand grinded before reaching 1 mm thickness and silver electrodes were deposited in both faces followed by heat treatment at 400°C during 15 minutes. The samples were then placed in a sample holder with silver electrodes to measure electrical current with applied voltage. Current-voltage curves were determined for different temperatures.

3. Results and discussions

Average grain size and densities of the sintered systems at the conditions described above are shown in Table I. The values for average grain sizes are larger than that for pure SnO_2 system [6]. For pure system the starting particle size is about 0.2 μm and after sintering at 1300°C for 3 h the grain size reaches values near 1.0 μm. In Table I, the average grain size reaches value between 5 and 7 μm.

TABLE I Relative density and mean grain size for the Ta_2O_5 doped SnO_2·CoO system sintered at 1300°C for 2 h

Ta_2O_5 concentration	Relative density (%)	Mean grain size (μm)
0.05	97.8	6.87
0.075	97.3	5.68

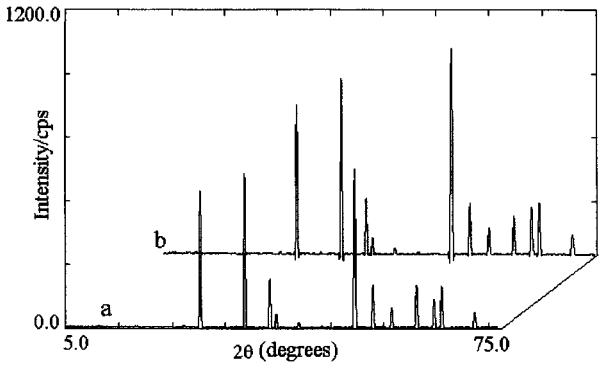

Figure 1 X-ray diffractograms for the $0.99SnO_2$·0.01CoO system containing two different Ta_2O_5 concentrations: a) 0.05 mol%; and b) 0.075 mol%.

Phase analysis by XRD in both systems considered in this study indicate only the crystalline phase of type rutile corresponding to SnO_2 (Fig. 1). However the additives concentrations used in this study were very small being bellow the XRD detection limit. Lattice parameters, determined by the least square method, showed small deviation of unit cell parameters a and c ($a = 4.737 \pm 0.003$ and $c = 3.185 \pm 0.002$). The SnO_2 structure is characterized to present interstitial vacant sites that allow the formation of solid solution. However, this phenomenon is not likely to occur since only small distortion in the SnO_2 lattice is observed with the addition of dopants. Moreover, the high observed densification in these systems can only be explained by the formation of extrinsic lattice defects due to substitution of Co^{2+} and/or Co^{3+} by the Sn^{4+} ions. This substitutional solid solution can be represented by the following equations:

$$CoO \xrightarrow{SnO_2} Co''_{Sn} + V_{\ddot{O}} + \frac{1}{2}O_2, \qquad (1)$$

$$Co_2O_3 \xrightarrow{SnO_2} 2Co'_{Sn} + V_{\ddot{O}} + \frac{3}{2}O_2. \qquad (2)$$

Then, if oxygen is the controlling species for diffusion, the formation of these defects promotes the densification of SnO_2 based ceramics.

The microstructures of the Ta_2O_5 doped SnO_2·CoO ceramics are shown in Figs 2 and 3. These micrographs show the presence of few trapped pores inside the grains or at the grain boundary. The increase of the Ta_2O_5

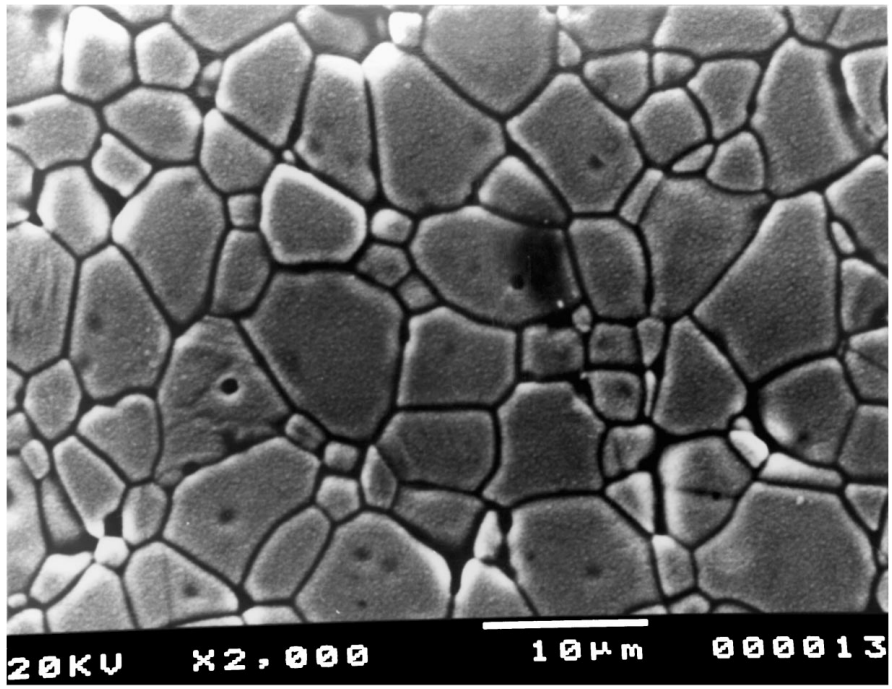

Figure 2 SEM micrograph of the 0.05 mol% Ta_2O_5 doped $0.99SnO_2$·0.01CoO system sintered at 1300°C for 2 h. The surface was thermally etched at 1250°C for 15 minutes.

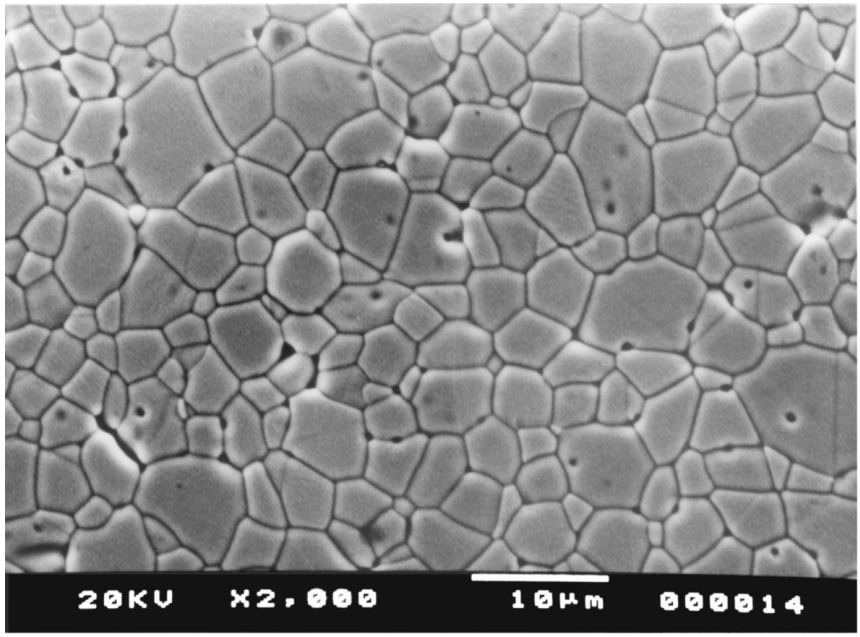

Figure 3 SEM micrograph of the 0.075 mol% Ta_2O_5 doped $0.99SnO_2{\cdot}0.01CoO$ system sintered at 1300°C for 2 h. The surface was thermally etched at 1250°C for 15 minutes.

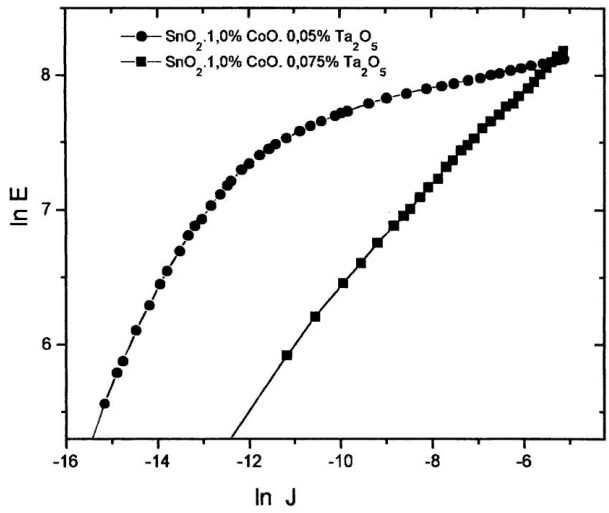

Figure 4 Characteristic $\ln E \times \ln J$ curves for the Ta_2O_5 doped $0.99SnO_2{\cdot}0.01CoO$ system sintered at 1300 °C for 2 h.

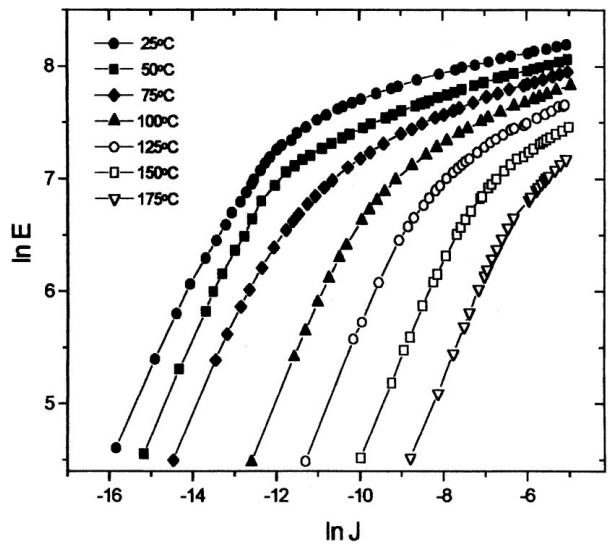

Figure 5 Characteristic $\ln E \times \ln J$ curves for the 0.05 mol% Ta_2O_5 doped $0.99SnO_2{\cdot}0.01CoO$ system sintered at 1300°C for 2 h and measured at different temperatures.

concentration leads to the decrease in the ceramic grain size.

The results of $\ln E$ versus $\ln J$ for the Ta_2O_5 doped $SnO_2{\cdot}CoO$ ceramics measured at room temperature are shown in Fig. 4. It is observed in this figure that the increase in the Ta_2O_5 concentration from 0.05 to 0.075 modifies substantially the electrical behavior of the $SnO_2{\cdot}CoO$ ceramics. Fig. 5 displays the characteristic $\ln E$ versus $\ln J$ curves, measured at different temperatures for the system containing 0.05 mol% of Ta_2O_5. As expected, the current leakage increase and the non linear coefficient α decrease with increasing temperature testing.

The varistor electrical behavior is governed by the presence of electrical barriers at the grain boundaries of the ceramic material. Then the electric field breakdown E_r depends on the average number of electrical barrier formed per unit length during sintering (n) and on the voltage barrier (v_b), which in ZnO based varistor is about 2 to 4 volts/barrier [16–18]. Thus the following equation relates v_b and E_r:

$$E_r = n v_b. \tag{3}$$

Considering that L is the thickness of the cylindrical sample, and d is the mean grain size, then Equation 3 can be given by:

$$E_r = \frac{L v_b}{d}. \tag{4}$$

Therefore, for the studied systems in this work, the increase on E_r with the decrease in d would be expected, keeping v_b constant. However, the results show that with the decrease in grain size the breakdown voltage

TABLE II Breakdown electric field (E_r), current leakage (I_l) nonlinear coefficient (α) and electric potential per barrier for the Ta_2O_5 doped SnO_2·CoO systems

Ta_2O_5 concentration	Measuring temp. (°C)	E_r (V/cm) at 1 mA/cm^2	I_l (A)	α	v_b (V/ barrier)
0.05	25	2940	1.3×10^{-6}	13.0	2.0
0.05	50	2660	2.4×10^{-6}	8.9	1.7
0.05	75	2320	5.7×10^{-6}	8.3	1.5
0.05	100	1910	3.3×10^{-5}	7.8	1.2
0.05	125	1550	1.1×10^{-4}	6.0	1.0
0.05	150	1040	3.8×10^{-4}	5.0	0.7
0.05	175	530	1.2×10^{-3}	2.9	0.3
0.075	25	1910	7.0×10^{-5}	3.0	1.1

decrease from 2940 to 1910, as observed in Table II. These results can be explained by the increase in the conductivity of the varistor system with increasing Ta_2O_5 from 0.05 to 0.075. Other explanation for the decrease in the E_r is that the number of effective barrier decreases with increasing amount of Ta_2O_5. The addition of Ta_2O_5 in SnO_2 produces similar effect as that of the Nb_2O_5 in the SnO_2·CoO·Nb_2O_5 system studied by Pianaro *et al.* [8].

These effects can be explained if one considers the following defect formation reactions:

$$2Ta_2O_5 \xrightarrow{SnO_2} 4\,Ta_{\dot{S}n} + V''''_{Sn} + 5O_2, \qquad (5)$$

$$V''''_{Sn} + 2\,V_{\ddot{O}} \rightarrow V^x_{Sn} + 2V^x_O, \qquad (6)$$

$$2O^x_O + V^x_{Sn} \rightarrow O_{2(g)} + 2\,V_{\ddot{O}} + V''''_{Sn}. \qquad (7)$$

As observed in Equation 5, Ta^{5+} can replace the Sn^{4+} ions producing tin vacancies. These vacancies could react with intrinsic SnO_2 oxygen vacancy annealing these defects as represented by Equation 6. Otherwise, SnO_2 lattice oxygen can react according to Equation 7, restoring the oxygen vacancies and producing tin vacancies [13].

The electrical behavior of the studied systems for low values of electrical field is similar (Fig. 4) and the electrical conduction is of the thermionic type. In this kind of emission the current density has an exponential dependence with temperature, according to the following equation [19]:

$$J = J_0 \exp\left(-\frac{E_a}{kT}\right) \qquad (8)$$

where J_0 is a constant, E_a is the activation energy for electron jump, k is the Boltzmann constant and T is the absolute temperature. Considering that the potential barriers are of Schottky type separated by thin film and that the conduction mechanism is by thermionic emission, the current density is related to the electric field, E, by the following equation [20]:

$$J_s = A^* T^2 \exp\left[\frac{-\left(\phi_b - \beta E^{\frac{1}{2}}\right)}{kT}\right], \qquad (9)$$

where A^* is the Richardson constant, ϕ_b is the electric potential barrier height formed at the interface region, E is the electric field and β is a constant related to the potential barrier width, ω. The constant β is given by:

$$\beta = \left[\left(\frac{1}{n\omega}\right)\left(\frac{2e^3}{4\pi\varepsilon_0\varepsilon_r}\right)\right]^{\frac{1}{2}}, \qquad (10)$$

where n is the number of grains per unit length, e is the electron charge, ε_0 and ε_r are the vacuum and material dielectric permitivities, respectively, n can be calculated by:

$$n = \frac{L}{d}, \qquad (11)$$

where L is the sample thickness and d is the mean grain size of SnO_2 varistor determined from the SEM micrograph.

The potential barriers can also be of the Poole-Frenkel type and thermal excitation of the trapped electrons in the acceptors states, located at the interface, is related to the electric field by the following equation:

$$J_{pf} = cE \exp\left[\frac{-\left(\phi_b - 2\beta E^{\frac{1}{2}}\right)}{kT}\right], \qquad (12)$$

where c is a material constant and the other parameters are the same as described in Equation 9.

The plot of ln J as function of $E^{1/2}$ for different temperatures of the 0.05 mol% doped 0.99SnO_2·0,01CoO system are shown in Fig. 6. For low values of E these curves are straight line and the extrapolation of these lines to $E = 0$ give the values of current density (J_0) for different temperatures as shown in Fig. 6b. The plot of ln J as function of $1/T$ is a straight line as represented in Fig. 7 and the slope of this curve gives the activation energy for electronic transport. The potential barrier height measured was 0.76 eV while the constant β was found to be 4.75×10^{-3} $V^{1/2}$ $cm^{1/2}$.

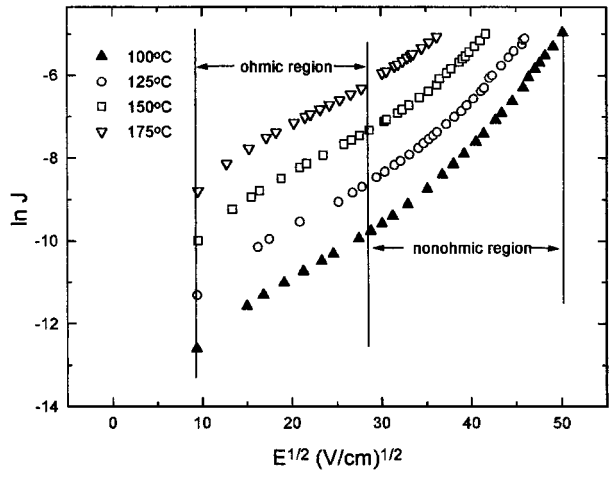

Figure 6 (a) Characteristic ln $J \times E^{1/2}$ curves for the 0.05 mol% Ta_2O_5 doped 0.99SnO_2·0.01CoO system sintered at 1300 °C for 2 h and measured at different temperatures; (b) Extrapolation of the ln $J \times E^{1/2}$ for $E = 0$.

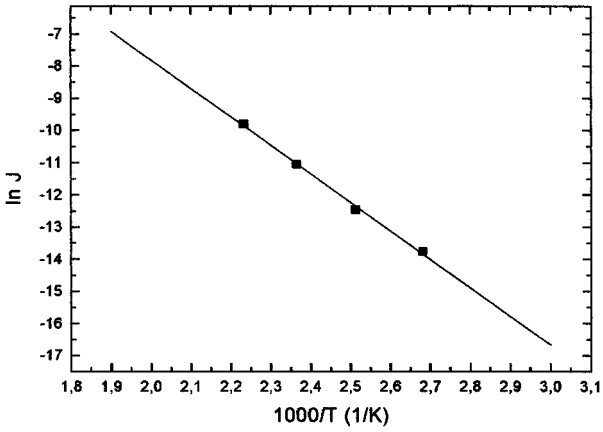

Figure 7 Curves of $\ln J \times 1/T$ for the 0.05 mol% Ta_2O_5 doped $0.99SnO_2{\cdot}0.01CoO$ system sintered at 1300°C for 2 h and measured at different temperatures.

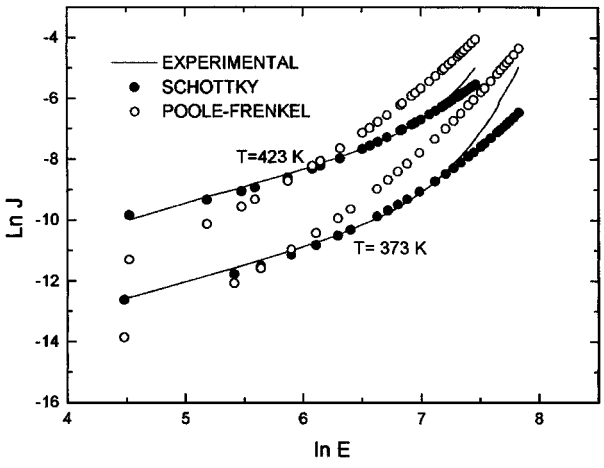

Figure 8 Plot of $\ln J$ versus $\ln E$ for the 0.05 mol% Ta_2O_5 doped $0.99SnO_2{\cdot}0.01CoO$ system sintered at 1300 °C for 2 h and measured at different temperatures. Comparison with the theoretical curves predicted by the Schottky and Poole-Frenkel models ($A_{373K} = 44.7$ A·cm^{-2} K^{-2}, $A_{423K} = 0.12$ A·cm^{-2} K^{-2}, $c_{373K} = c_{423K} = 54.6$ A·cm^{-1} V^{-1}).

To verify the electric conduction mechanism at low current densities, the Equations 9 and 12 were plotted and compared with the experimental data in the Fig. 8. As observed in this figure the best fits for the experimental data follow the Schottky type potential barrier. This agreement occurs only in the region where the electric conductivity is dependent on the temperature. For higher electric fields where $J > 1$ mA/cm^2 the curves have the tendency to converge in a single point. For this region the conduction is affected by the distortion of the potential electric barrier, resulting in a decrease in its height, which facilitates the electronic transport.

The origin of the non linear behavior of the CoO and Ta_2O_5 doped SnO_2 ceramics can be explained by the defect formation given in Equations 1, 2, 5, 6 and 7. Then, in analogy to the atomic defect model proposed by Gupta and Carlson [21] for ZnO based varistor, a similar model for SnO_2 based ceramics can be proposed as represented in Fig. 9. Then, in this model, the negative charges at the interface came from tin vacancies V''''_{Sn} and cations substitution such as Co''_{Sn}. These electric charges are balanced by positive charges distributed within a region with a distance ω from the

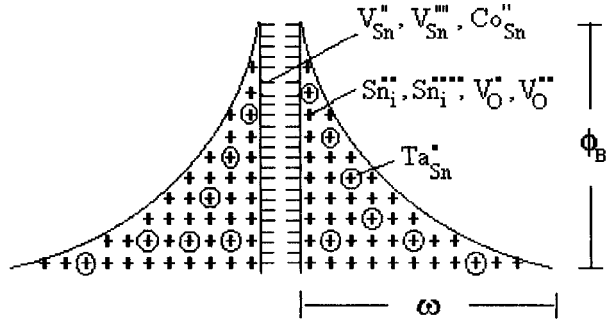

Figure 9 Atomic defect model proposed to explain the potential barrier formation at the grain boundary of SnO_2 varistor system.

interface. These positive charges are oxygen vacancies ($V_{\ddot{O}}$) and/or interstitial tin ions $Sn_i^{\cdot\cdot\cdot\cdot}$, as well as other positive defects such $Ta_{\dot{S}n}$ promoted by substitutional solid solution. Then the system $SnO_2{\cdot}CoO{\cdot}Ta_2O_5$, similar to ZnO based varistor, can be characterized by the existence of low resistivity grains separated by high electric resistivity boundaries.

4. Conclusions

The addition of 0.05 mol% of Ta_2O_5 to the $0.99SnO_2{\cdot}0.01CoO$ system produced a varistor behavior with a high non-linear coeficient ($\alpha = 13$). Increasing the Ta_2O_5 concentration to 0.075 mol% decrease grain size and promotes a dramatic increase in the leakage current and decrease in the non-linear coefficient. This electric non-linear behavior is explained by the formation of atomic defects that are responsible for the formation of an electric potential barrier at the grain boundaries. A Schottky type potential barrier was found to better represent the electronic emission transport at the linear pre-breakdown region (low E values). The measured potential barrier height was 0.76 eV.

References

1. Z. M. JARZEBSKI and J. P. MARTON, *J. Electrochem. Soc.* **123** (1976) 299C.
2. J. A. VARELA, *Cerâmica* **31** (1985) 241.
3. J. F. MCALER, P. T. MOSELEY, J. O. W. NORRIS and D. E. WILLIAMS, *J. Chem. Soc. Faraday Trans.* **83** (1987) 1323.
4. J. A. VARELA, O. J. WHITTEMORE and E. LONGO, *Ceram. Intern.* **16** (1990) 177.
5. J. A. CERRI, E. R. LEITE, D. GOUVÊA, E. LONGO and J. A. VARELA, *J. Am. Ceram. Soc.* **79**(3) (1996) 799.
6. T. KIMURA, S. INADA and T. YAMAGUCH, *J. Mater. Sci.* **24** (1989) 220.
7. M. K. PARIA and H. S. MAITI, *ibid.* **18** (1983) 2101.
8. S. A. PIANARO, P. R. BUENO, E. LONGO and J. A. VARELA, *J. Mater. Sci. Letters* **14** (1995) 692.
9. S. A. PIANARO, P. R. BUENO, P. OLIVI, E. LONGO and J. A. VARELA, *ibid.* **16** (1997) 634.
10. S. A. PIANARO, E. C. PEREIRA, L. O. S. BULHÕES, E. LONGO and J. A. VARELA, *J. Mater. Sci.* **30** (1995) 133.
11. W. G. MORRIS, *J. Vac. Sci. Technol.* **13** (1976) 926.
12. J. WONG, *J. Appl. Phys.* **47** (1976) 4971.
13. W. C. LAS, N. DOLET, P. DORDOR and J. P. BONNET, *ibid.* **74** (1993) 6191.
14. A. C. ANTUNES, S. R. M. ANTUNES, S. A. PIANARO, M. R. ROCHA, E. LONGO and J. A. VARELA, *J. Mater. Sci. Letters*, accepted.
15. M. I. MENDELSON, *J. Am. Ceram. Soc.* **52**(8) (1969) 443.

16. L. M. LEVINSON and H. R. PHILIPP, *J. Appl. Phys.* **46**(3) (1975) 1332.
17. L. F. LOU, *ibid.* **50**(1) (1979) 555.
18. G. D. MAHAN, L. M. LEVINSON and H. R. PHILIPP, *J. Appl. Phys. Lett.* **33**(9) (1978) 830.
19. S. M. SZE, "Physics of Semiconductor Devices" (Wiley, New York, 1985).
20. K. EDA, *J. Appl. Phys.* **49** (1978) 2964.
21. T. K. GUPTA and W. G. CARLSON, *J. Mater. Sci.* **20** (1985) 3487.

Received 7 April 1998
and accepted 30 September 1999